ChemComm

Improving stability of the metal-free primary energetic cyanuric triazide (CTA) through cocrystallization

Journal:	*ChemComm*
Manuscript ID	CC-COM-12-2019-009465.R1
Article Type:	Communication

COMMUNICATION

Improving stability of the metal-free primary energetic cyanuric triazide (CTA) through cocrystallization

Leila M. Foroughi,[a] Ren A. Wiscons,[a] Derek R. Du Bois,[a] and Adam J. Matzger*[a,b]

Received 00th January 20xx,
Accepted 00th January 20xx

DOI: 10.1039/x0xx00000x

Cyanuric triazide (CTA) and benzotrifuroxan (BTF) form a metal-free primary energetic cocrystal with suppressed volatility and improved thermal properties relative to CTA. Though electrostatic potential maps of the most stable conformations do not predict favorable interactions, a higher energy conformer has appropriate electrostatics and is selected by BTF in the cocrystal.

The environmental and health concerns associated with the continued use of heavy metal containing impact sensitive (primary) explosives motivate development of "green energetics" that lack toxic metals such as lead and mercury.[1–3] The use of lead in energetics has become highly regulated with restrictions enacted to reduce environmental release.[1,2,4] As a result it is a priority to identify replacements for lead azide (Chart 1), a commonly used primary, that are easily synthesized, inexpensive, thermally stable, and show competitive, if not improved, explosive performance compared to current heavy metal containing formulations.[1,5,6] Primary energetics are generally used to initiate the detonation of secondary energetics, more powerful and less sensitive materials (e.g. HMX, RDX, TNT), and must show sensitivity to outside stimuli such as impact or heat. The vast majority of alternatives for lead azide have been hampered by limitations in thermal stability,[7,8] complicated synthetic procedures, or safety concerns.[3,9] Among newly developed primaries are a copper-containing nitro-tetrazolate salt (DBX-1[10,11]), and the potassium salt dinitraminobistetrazolate (K_2DNABT),[12] both shown in Chart 1. Potential hygroscopicity and hydrate formation often plague salt-based energetics. A neutral energetic compound identified as a potential replacement primary is cyanuric triazide (CTA),

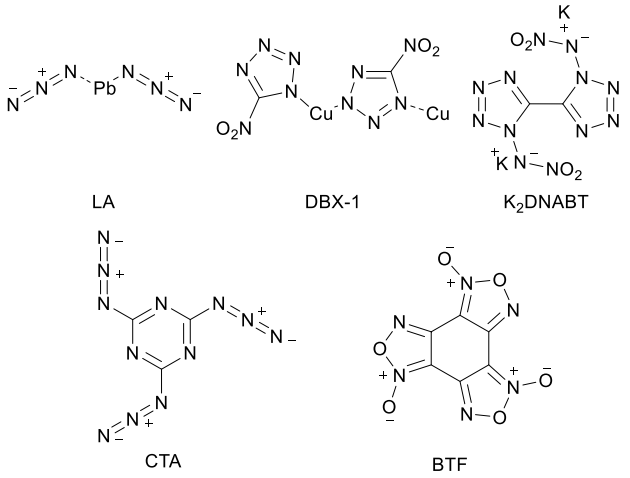

Chart 1. Molecular structures of some primary energetics and the secondary energetic coformer benzotrifuroxan.

also known as 2,4,6-triazidotriazine. CTA (Chart 1) is a promising candidate as a green primary energetic and is more powerful than lead azide;[13] CTA can be synthesized in nearly quantitative yield in a single chemical transformation from inexpensive commercially available starting materials.[3,13] However, concerns about the thermal/impact sensitivity of CTA[1,6,14] and volatility under ambient conditions,[13,15] have limited its broad application.

Cocrystallization has recently been used to alter the thermal stability, sensitivity, corrosivity, and volatility of energetic species.[16–24] However, cocrystal formation between two species is rarely guaranteed and identifying energetic compounds that can cocrystallize is particularly challenging because energetics often lack functional groups that participate in directional and complementary intermolecular interactions (such as hydrogen bonding) that encourage cocrystal formation. For this reason, electrostatic potential maps have become a valuable tool for identifying molecules and/or functional groups likely to form

[a] *Department of Chemistry, Macromolecular Science and Engineering Program, University of Michigan, 930 North University Avenue, Ann Arbor, MI 48109-1055, United States*
[b] *Macromolecular Science and Engineering Program, University of Michigan, 930 North University Avenue, Ann Arbor, MI 48109-1055, United States*

† Electronic supplementary information (ESI) available: Synthesis and characterization of the cocrystal. CCDC: 1969834 and 1969835. For ESI and crystallographic data in CIF see DOI: ----------

favourable electrostatic interactions in systems where interaction modes between two distinct species are not evident.[25,26]

Herein, electrostatic potential maps are used to identify an energetic coformer for CTA that leads to a CTA-based primary energetic cocrystal showing suppressed volatility and improved detonation performance while maintaining high sensitivity to impact. The hydrogen free secondary energetic benzotrifuroxan (BTF) was selected as a cocrystallization candidate due to previous reports that the material has relatively high sensitivity to impact compared to other secondary energetics[27,28] and has previously been used to successfully form energetic cocrystals with other coformers.[22,29]

In order to evaluate the likelihood that a cocrystal could form between these two compounds, electrostatic potential maps were calculated and the regions of maximum electrostatic potential ($V_{s,max}$) and minimum electrostatic potential ($V_{s,min}$) were compared for BTF (Fig. 1a) and two conformers of CTA (Fig. 1b), the C_{3h} conformation, exhibited in the crystal structure of pure CTA,[30,31] and the theoretical C_s conformer examined by Rocha and coworkers.[32] Both the $V_{s,min}$ and $V_{s,max}$ are calculated to be greater in magnitude for the C_s conformer (-158.7 kJ mol^{-1} and 120.7 kJ mol^{-1}) than for the C_{3h} conformer (-115.8 kJ mol^{-1} and 114.7 kJ mol^{-1}), indicating that the CTA C_s is more polarized and capable of forming more favourable intermolecular interactions. The calculated $V_{s,min}$ and $V_{s,max}$ values for BTF are -87.6 kJ mol^{-1} and 197.3 kJ mol^{-1}, suggesting that the strongest intermolecular interactions would be between the most electron-rich site on CTA C_s and the most electron deficient site on BTF. Additionally, an energy profile was calculated to evaluate the accessibility of CTA C_s and to identify the transition state energy. Optimized geometries for CTA C_{3h}, the transition state, and C_s were used to determine the rotational barrier and relative distribution between CTA C_{3h} and C_s conformers. The C_s conformer is 0.3 kcal mol^{-1} higher in energy than the C_{3h} conformer and the interconversion barrier is approximately 11.7 kcal mol^{-1}, a barrier traversable at room temperature and consistent with that determined by Rocha and coworkers.[32] These results emphasize the importance of considering all accessible conformers, and not exclusively the equilibrium geometry, when calculating electrostatic potential maps as guides to cocrystal design.

Initial attempts to cocrystallize CTA and BTF were performed by fusion of the CTA melt in the presence of solid BTF, producing blade-like crystals that show a unique Raman spectrum from those of the pure coformers. The cocrystal is also accessible via solvent-mediated slurry conversion of a 1:1 mixture of CTA and BTF in a 50/50 by volume isooctane/toluene solution at room temperature, resulting in a bulk phase that is 2:1 CTA/BTF cocrystal (excess BTF remains in the mother liquor). The room temperature crystal structure was obtained using a crystal grown by fusion and a crystal grown from slurry was used to obtain the low temperature crystal structure.

The cocrystal formed between CTA and BTF was analysed using single crystal X-ray diffraction at room temperature and 100 K (ESI†). The cocrystal solves in the *C*2/*c* space group with one molecule of CTA and a half molecule of BTF in the asymmetric unit. CTA adopts the C_s conformer in contrast to the C_{3h} conformer present in the crystal structure of pure CTA. Each molecule of BTF is flanked by two molecules of CTA, interacting with opposite faces of BTF through T-shaped interactions and forming trimers, consistent with electrostatic potential map analysis. The two T-shaped π-interactions for each molecule of BTF are related by a 2-fold axis that bisects BTF with a closest interaction distance of 2.959 Å between an aromatic nitrogen of the triazine ring and the centroid of the BTF molecule (Fig. 2a). The 2-fold axis also forces disorder of BTF over two positions, which is well-defined at low temperature and shows thermal ellipsoids elongated in the plane of the BTF molecule at room temperature, suggesting additional thermal motion. In both orientations of BTF in the low temperature cocrystal structure, multiple close contacts are formed between the BTF furoxan rings and the CTA azido groups of neighbouring trimers (Fig. 2b) albeit at distances that cannot be precisely defined due to disorder.

To determine the impact sensitivity of CTA and the 2:1 CTA/BTF cocrystal, small scale impact testing was deployed. In this method, 2 mg of each sample were placed in a non-hermetic DSC pan, and a 5 lb weight was dropped onto the pan from premeasured distances using our in-house apparatus (see ESI†).[33] Over forty drops were performed to determine the

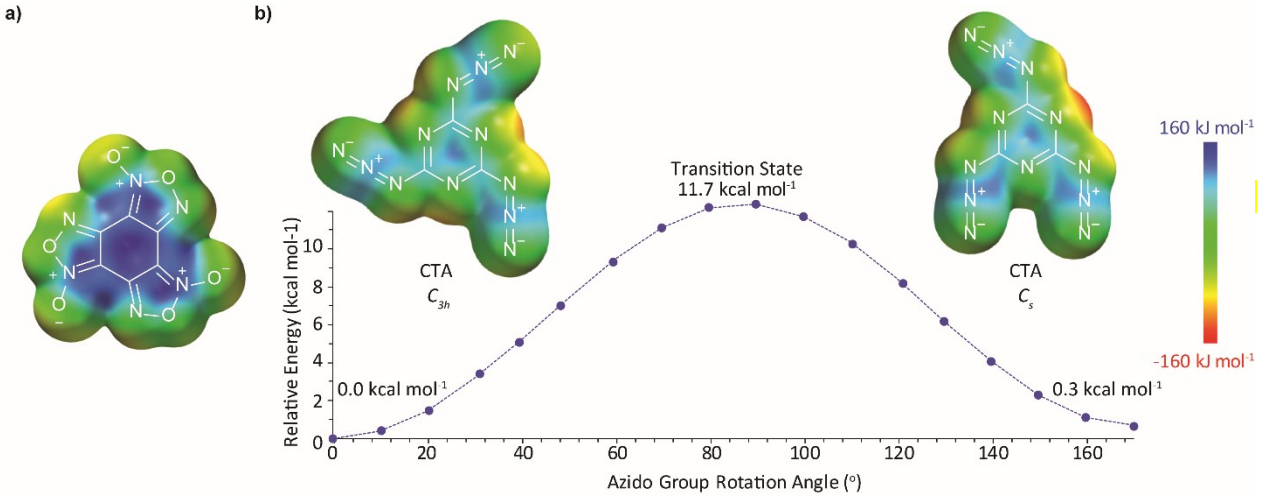

Fig. 1 (a) Electrostatic potential maps calculated using B3LYP/6-311G** for CTA conformers C_{3h} and C_s, and the coformer BTF, with a shared scale representing the surface potential in kJ mol^{-1}. (b) An energy profile was calculated using (B3LYP/6-311G(d)) for rotation around the C–N_3 bond relating the C_{3h} and C_s conformers to identify the transition state geometry. The geometries for CTA C_{3h}, the transition state, and C_s were optimized using (MP2/6-311G(d,p)) and the rotational barrier was determined using those energies.

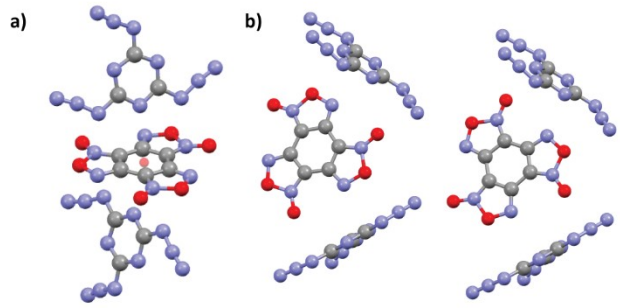

Fig. 2 Packing of CTA and BTF in the 2:1 crystal structure. For clarity, the disorder of BTF is not shown and only one occupancy is present. (a) View of the C_s conformer of CTA interacting with the centroid in BTF from the crystal structure. b) View of a tape of BTF connected by interactions between the furazan ring and the nitrogen atoms of the azide group.

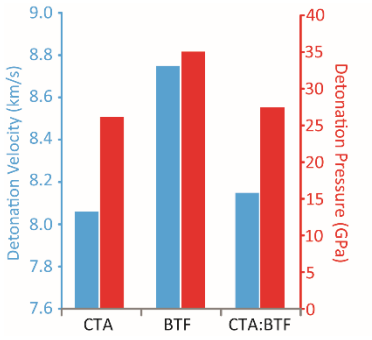

Fig. 3 Graph comparing the calculated detonation velocity (blue) and detonation pressure (red) of CTA, BTF, and the cocrystal. Values were predicted using the thermochemical code Cheetah 7.0.

height at which there is a 50% probability of detonation (Dh_{50}).[34] The drop height values were compared to Pentaerythritol tetranitrate (PETN), a secondary energetic that is commonly used to differentiate the impact sensitivities of primary (Dh_{50} heights below PETN) and secondary energetics (Dh_{50} heights above PETN). The impact sensitivity of the cocrystal is 19 cm, less sensitive than CTA (Dh_{50} = 12 cm), yet more sensitive than PETN (Dh_{50} = 21 cm)[35]; based on impact sensitivity, CTA/BTF is a primary energetic that is less sensitive than CTA. This decrease in sensitivity is advantageous, because the high sensitivity of CTA has been previously cited as a concern in using CTA as a replacement for lead azide.[14] The detonation performance of the CTA/BTF cocrystal was evaluated and compared to its constituents (Fig. 3). In addition to having a detonation velocity and detonation pressure slightly higher than CTA, the cocrystal shows a slight increase in density relative to CTA (cocrystal: 1.737 g cm^{-3}; CTA: 1.723 g cm^{-3} [36]).

The thermal behaviour of CTA/BTF was characterized using differential scanning calorimetry (DSC) and thermogravimetric analysis (TGA). The DSC traces indicate melting onset temperatures of 94, 143, and 196 °C for CTA, the cocrystal, and BTF, respectively (Fig. 4a and ESI†). The increased onset temperature for the CTA/BTF melt event relative to CTA demonstrates the stabilizing impact of interactions present in the cocrystal; two decomposition events are observed (~178 °C and 250 °C) which are similar to those of pure CTA (~175 °C) and BTF (~243 °C) and not shifted to significantly higher temperatures as has been recently observed for some cocrystals.[18,37] The TGA traces of CTA, the cocrystal, and BTF also show weight loss in two events, the first one starting at a temperature approximately 25 °C higher than that of CTA and the second event occurring at a very similar temperature to BTF (Fig. 4b). However, the steps do not correspond to clean loss of individual components as evidenced by the observation of vibrational bands associated with CTA in samples heated to 180 °C.

The propensity of CTA to sublime has hampered its application and this property is evident in the TGA traces (open pan, Fig. 4b) which show significant mass loss prior to the decomposition temperature of CTA (closed pan DSC, Fig. 4a). To investigate whether cocrystallization leads to a decrease in CTA volatility, the rate of CTA mass loss was quantified through isothermal TGA experiments with CTA and the CTA/BTF cocrystal. These experiments were carried out in a hermetically-sealed aluminium DSC pan with a hole (r ≅ 330 μm) in the lid. The rate of mass loss as a function of time, *dm/dt*, was determined at 85, 100, and 115 °C (See ESI†). The rate of mass loss for the cocrystal relative to CTA was 7.6, 7.1, and 5.3 times lower at 85, 100, and 115 °C respectively. Thus, the volatility of CTA is suppressed significantly through cocrystallization.

In summary, we present a primary energetic cocrystal formed between CTA and BTF. Electrostatic potential maps and an energy profile of both dominant conformers of CTA led to the prediction that the electron rich area of CTA C_s would be able to interact favourably with the electron deficient π region of BTF. The resulting cocrystal has a much higher melting point, significantly lower volatility, and less impact sensitivity (while still qualifying as a primary) relative to CTA. This work emphasizes the utility of cocrystallization as a means to alter energetic properties and presents a strategy for identifying

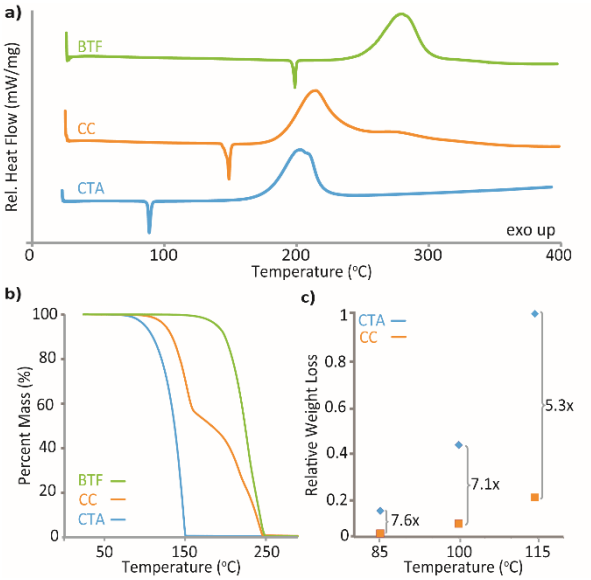

Fig. 4 (a) DSC thermograms showing the melting point and decomposition behaviour of BTF, the cocrystal, and CTA (b) TGA traces of BTF, cocrystal, and CTA. (c) Relative weight loss from sublimation of CTA and the cocrystal measured using TGA (see ESI†).

green primary energetics based on compounds that have been deemed too unstable for broad application.

The authors acknowledge the support of the Army Research Office (ARO) in the form of a Multidisciplinary University Research Initiative (MURI) (grant number: W911NF-13-1-0387).

Conflicts of interest

There are no conflicts to declare.

Notes and References

‡ The efficacy of initiating a secondary explosive with a primary requires large-scale testing. This has recently been reported for several novel energetics.[38–40]

1 M. H. V. Huynh, M. A. Hiskey, T. J. Meyer and M. Wetzler, *Proc. Natl. Acad. Sci. U. S. A.*, 2006, **103**, 5409–5412.
2 T. Brinck, Ed., *Green energetic materials*, John Wiley & Sons Inc, Chichester, West Sussex, United Kingdom, 2014.
3 J. J. Sabatini and K. D. Oyler, *Crystals*, 2016, **6**, 5 (1-22).
4 J. Giles, *Nature*, 2004, **427**, 580–581.
5 N. Mehta, K. Oyler, G. Cheng, A. Shah, J. Marin and K. Yee, *Z. Anorg. Allg. Chem.*, 2014, **640**, 1309–1313.
6 R. Matyáš and J. Pachman, *Primary Explosives*, Springer Berlin Heidelberg, Berlin, Heidelberg, 2013.
7 M. Kaiser and U. Ticmanis, *Thermochim. Acta*, 1995, **250**, 137–149.
8 D. J. Whelan, R. J. Spear and R. W. Read, *Thermochim. Acta*, 1984, **80**, 149–163.
9 T. M. Klapötke and T. Wloka, *Peroxide Explosives*, John Wiley & Sons, Ltd., Chichester, 2014.
10 D. D. Ford, S. Lenahan, M. Jörgensen, P. Dubé, M. Delude, P. E. Concannon, S. R. Anderson, K. D. Oyler, G. Cheng, N. Mehta and J. S. Salan, *Org. Process Res. Dev.*, 2015, **19**, 673–680.
11 J. W. Fronabarger, M. D. Williams, W. B. Sanborn, J. G. Bragg, D. A. Parrish and M. Bichay, *Propellants, Explos., Pyrotech.*, 2011, **36**, 541–550.
12 D. Fischer, T. M. Klapötke and J. Stierstorfer, *Angew. Chem., Int. Ed.*, 2014, **53**, 8172–8175.
13 R. Meyer, J. Köhler and A. Homburg, *Explosives*, Wiley-VCH, Weinheim, 5th ed., 2002.
14 W. R. Tomlinson and O. E. Sheffield, *Engineering Design Handbook: Explosives Series Properties of Explosives of Military Interest*, Army Materiel Command, Alexandria, VA, 1971.
15 B. L. Korsunskiy, V. V. Nedel'ko, V. V. Zakharov, N. V. Chukanov, A. D. Chervonnyi, T. S. Larikova and S. V. Chapyshev, *Propellants, Explos., Pyrotech.*, 2017, **42**, 123–125.
16 Y. Tan, Z. Yang, H. Wang, H. Li, F. Nie, Y. Liu and Y. Yu, *Cryst. Growth Des.*, 2019, **19**, 4476–4482.
17 K. B. Landenberger, O. Bolton and A. J. Matzger, *J. Am. Chem. Soc.*, 2015, **137**, 5074–5079.
18 J. C. Bennion, Z. R. Siddiqi and A. J. Matzger, *Chem. Commun.*, 2017, **53**, 6065–6068.
19 C. B. Aakeröy, T. K. Wijethunga and J. Desper, *Chem. Eur. J.*, 2015, **21**, 11029–11037.
20 O. Bolton and A. J. Matzger, *Angew. Chem., Int. Ed.*, 2011, **50**, 8960–8963.
21 N. Liu, B. Duan, X. Lu, H. Mo, F. Bi, B. Wang, J. Zhang and Q.-L. Yan, *Propellants, Explos., Pyrotech.*, **44**, 1242–1253.
22 H. Zhang, C. Guo, X. Wang, J. Xu, X. He, Y. Liu, X. Liu, H. Huang and J. Sun, *Cryst. Growth Des.*, 2013, **13**, 679–687.
23 C. Guo, H. Zhang, X. Wang, X. Liu and J. Sun, *J. Mater. Sci.*, 2013, **48**, 1351–1357.
24 S. R. Kennedy and C. R. Pulham, in *Co-crystals*, eds. C. B. Aakeröy and Sinha, A. S., CPI Group (UK) Ltd, Croydon, 2018, pp. 231–266.
25 K. B. Landenberger and A. J. Matzger, *Cryst. Growth Des.*, 2010, **10**, 5341–5347.
26 R. V. Kent, R. A. Wiscons, P. Sharon, D. Grinstein, A. A. Frimer and A. J. Matzger, *Cryst. Growth Des.*, 2018, **18**, 219–224.
27 H. H. Cady, A. C. Larson and D. T. Cromer, *Acta Cryst.*, 1966, **20**, 336–341.
28 X. Huang, Z. Qiao, X. Dai, K. Zhang, Y. Wen, M. Li and F. Guo, *Chem. Phys. Lett.*, 2019, 136861.
29 Z. Yang, Y. Wang, J. Zhou, H. Li, H. Huang and F. Nie, *Propellants, Explos., Pyrotech.*, 2014, **39**, 9–13.
30 I. E. Knaggs, *Proc. R. Soc. London, Ser. A*, 1935, **150**, 576–602.
31 E. Keßenich, T. M. Klapötke, J. Knizek, H. Nöth and A. Schulz, *Eur. J. Inorg. Chem.*, 1998, **1998**, 2013–2016.
32 A. Hammerl, T. M. Klapötke and R. Rocha, *Eur. J. Inorg. Chem.*, 2006, **2006**, 2210–2228.
33 J. C. Bennion, N. Chowdhury, J. W. Kampf and A. J. Matzger, *Angew. Chem., Int. Ed.*, 2016, **128**, 13312–13315.
34 W. J. Dixon and A. M. Mood, *J. Am. Stat. Assoc.*, 1948, **43**, 109–126.
35 R. V. Kent, T. P. Vaid, J. A. Boissonnault and A. J. Matzger, *Dalton Trans.*, 2019, **48**, 7509–7513.
36 C. R. Groom, I. J. Bruno, M. P. Lightfoot and S. C. Ward, *Acta Crystallogr., Sect. B: Struct. Sci.*, 2016, **72**, 171–179.
37 M. K. Bellas and A. J. Matzger, *Angewandte Chemie International Edition*, 2019, **58**, 17185–17188.
38 D. Fischer, T. M. Klapötke and J. Stierstorfer, *Angew. Chem., Int. Ed.*, 2015, **54**, 10299–10302.
39 M. Deng, Y. Feng, W. Zhang, X. Qi and Q. Zhang, *Nat Commun*, 2019, **10**, 1–8.
40 Q. Wang, X. Feng, S. Wang, N. Song, Y. Chen, W. Tong, Y. Han, L. Yang and B. Wang, *Adv. Mater.*, 2016, **28**, 5837–5843.